Earth's Future

RESEARCH ARTICLE
10.1029/2020EF001731

Key Points:
- The area affected by dry extremes has significantly increased (~1% per decade) during 1951–2015 in India
- Climate models project increase in the combined area affected by the dry and wet extremes in India (25–30%) by the end of the 21st century
- The population exposed to the dry and wet extremes is likely to increase threefold under a (2°C) warmer world climate

Supporting Information:
- Supporting Information S1

Correspondence to:
R. Kumar and V. Mishra,
rohini.kumar@ufz.de;
vmishra@iitgn.ac.in

Citation:
Kumar, R., & Mishra, V. (2020). Increase in population exposure due to dry and wet extremes in India under a warming climate. *Earth's Future*, *8*, e2020EF001731. https://doi.org/10.1029/2020EF001731

Received 30 JUL 2020
Accepted 27 OCT 2020
Accepted article online 5 NOV 2020
Corrected 2 JAN 2021

This article was corrected on 2 JAN 2021. See the end of the full text for details.

Increase in Population Exposure Due to Dry and Wet Extremes in India Under a Warming Climate

Rohini Kumar[1] and Vimal Mishra[2,3,4]

[1]Helmholtz Centre for Environmental Research – UFZ, Leipzig, Germany, [2]Civil Engineering, Indian Institute of Technology (IIT) Gandhinagar, Gandhinagar, Gujarat, India, [3]Earth Sciences, Indian Institute of Technology (IIT) Gandhinagar, Gandhinagar, Gujarat, India, [4]Kiran C. Patel Center of Sustainable Development, IIT Gandhinagar, Gandhinagar, Gujarat, India

Abstract Dry and wet extremes affect agricultural production, infrastructure, and socioeconomic well-being of about 1.4 billion people in India. Despite the profound implications of dry and wet extremes, their changes in the observed and projected climate in India are not well quantified. Here, using the observations from multiple sources, we show that the area affected by dry extremes during the monsoon season (June–September) and water-year (June–May) has significantly increased (~1% per decade; p value < 0.05) over the last six decades (1951–2015) in India. On the other hand, the area affected by wet extremes does not exhibit any significant trend over the same time period. Dry and wet extremes in the monsoon season are corroborated with the positive phase and negative phase of the sea surface temperature (SST) anomalies in the tropical Pacific Ocean (Niño 3.4 region). Global climate models (GCMs) project an increase of more than 25–30% (±3–6%) in the combined area affected by the dry and wet extremes in India by the end of the 21st century. The frequency of both dry and wet extreme years is also projected to increase in the majority of India (>80%) under a warmer world if the global mean temperature rises above 1.5°C (or 2°C) from a preindustrial level. Moreover, the population exposed to the dry and wet extremes is likely to increase threefold under the projected 2°C warmer world. Therefore, limiting global mean temperature rise below 2°C can substantially reduce the area and population exposure due to dry and wet extremes in India.

1. Introduction

Hydroclimatic extremes with long-lasting impacts and damages have increased in the observational record (Singh et al., 2014, 2019) and are likely to increase further under a warming climate (Mukherjee & Mishra, 2018; Perkins et al., 2012). Floods and droughts are the two hydroclimatic extremes that pose tremendous pressure on human society affecting crop production (Lesk et al., 2016; Lobell & Field, 2007; Peng et al., 2004), water availability (Barnett et al., 2005; Immerzeel et al., 2010; Piao et al., 2010; Schewe et al., 2014), and infrastructure (Hallegatte et al., 2013; Winsemius et al., 2016). Recent floods have shown that a single event can affect multiple countries posing risks to several aspects of human lives (Jongman et al., 2014).

Changes in the flood frequency, magnitude, and timings have been observed in many regions across the globe (Alfieri et al., 2015; Berghuijs et al., 2017; Gudmundsson et al., 2019; Huntingford et al., 2014; Ward et al., 2013). Such extreme events have affected millions of people in the past, and the human losses and economic damages from flooding are projected to rise substantially under a warming climate (Dottori et al., 2018). Moreover, both observations and model simulations show that droughts have also increased under the warming climate (Cook et al., 2015; Dai, 2013; Diffenbaugh et al., 2015; Trenberth et al., 2014).

India experiences both dry and wet extremes (Ali et al., 2019; Mishra et al., 2019; Singh et al., 2014, 2019), which cause severe economic, social, and environmental losses (Parida 2020; Parida et al., 2020; Udmale et al., 2015). Moreover, dense population and agriculture-based economy make India vulnerable due to high exposure to the hydroclimatic extremes (Krishna Kumar et al., 2004; Mishra et al., 2017). Dry and wet extremes have become frequent in India during the recent decades due to erratic monsoon and warming climate (Goswami et al., 2006; Mishra et al., 2012; Roxy et al., 2015, 2017; Singh et al., 2019). For instance, India has witnessed devastating floods in Uttarakhand (2013), Kashmir (2014), Chennai (2015), Gujarat (2017), Kerala (2018), Maharashtra (2019), Assam (2020), and Bihar (2020) that caused the loss of human lives and damage to agriculture and infrastructure (Kumar & Acharya, 2016; Ray et al., 2019).

Ray et al. (2019) reported that the recent floods in India occurred due to different atmospheric circulations and under different geomorphological settings. However, since precipitation extremes are projected to rise under the warming climate in India (Goswami et al., 2006; Mukherjee et al., 2018), extreme precipitation and initial hydrological conditions might have played a considerable role (Garg & Mishra, 2019; Sharma et al., 2018). Similarly, India has experienced notable droughts during the recent decades that have had an imprint on agriculture, and surface and groundwater resources (Mishra et al., 2019, 2020). Despite the profound implications of dry and wet extremes under the warming climate, the observed and projected changes in the area and the human population affected by these hydro-climatic extremes remain poorly understood.

Here, we provide a comprehensive assessment of the changes in the frequency, area, and population exposure affected by both dry and wet extremes in India under the warming climate. Our analysis encompasses both observed records and future projections based on multiple observational data sets and CMIP5 simulations of Global Climate Models (GCMs; Taylor et al., 2012) under two future scenarios (RCP 4.5 and 8.5). We also use projected demographic changes under different Shared Socioeconomic Pathways (SSPs; O'Neill et al., 2017; van Vuuren et al., 2014). Specifically, we analyze the projected changes in areal extents and occurrence of the dry and wet extremes as well the population exposure across India under different warming level scenarios. Our study also includes assessment on the projected changes under 1.5°C and 2°C global warming levels, which is in-line with the targeted temperature thresholds discussed in the 2015 Paris Agreement (UNFCC, 2015). To this end, we aim to address the following questions: (1) to what extent the spatial coverage and occurrence of dry and wet extremes in India are projected to change under different warming levels? And (2) how do the human population exposure to dry and wet extremes differ under different warming worlds?

2. Data and Methods

2.1. Data Sets

We used Standardized Precipitation-Evapotranspiration Index (SPEI; Vicente-Serrano et al., 2010) to identify dry and wet extremes that account for both atmospheric water availability and demand (i.e., precipitation and evapotranspiration; elaborated below in section 2.2). In India, the monsoon season rainfall contributes to approximately 80% of the total annual rainfall and is the predominant water source for the majority of Indian regions (Mishra et al., 2012). According to the India Meteorological Department (IMD), a deviation of 10% from the long-term mean rainfall is regarded as the monsoon rainfall surplus or deficit (Krishnamurthy & Shukla, 2000) leading to substantial areas being under wet or dry extremes, respectively. Recently, there have been concerns on the uncertainty of the observational data sets used to estimate the changes in Indian summer monsoon rainfall (Lin & Huybers, 2019; Singh et al., 2019). We, therefore, used four different observation-based gridded data sets in our analysis, which are available from the India Meteorological Department (IMD; Pai et al., 2014), Global Precipitation Climatology Centre (GPCC; Becker et al., 2013; Schneider et al., 2018), Climatic Research Unit (CRU; v4.02; Harris & Jones, 2019; Harris et al., 2020), and University of Delaware (UDEL; v5.01; Legates & Willmott, 1990). These data sets employ different methods and underlie station information to construct the gridded precipitation and temperature products. These observational products have been used in the past for analyzing rainfall characteristics across India (Jin & Wang, 2017; Roxy et al., 2015, 2017; Singh et al., 2014). The atmospheric water demand required was estimated using the potential evapotranspiration (PET; Vicente-Serrano et al., 2010). We used the Hargreaves and Samani (1985) method to estimate PET based on maximum and minimum air temperatures. The choice of the PET method is based on (limited) data availability over the observational period and following the recommendation by FAO to use this method in the absence of several variables that are required to estimate Penman-Monteith based PET (Allen et al., 1998). Using these precipitation and PET data sets, we estimated SPEI and analyzed the historical changes in wet and dry extremes across India since the mid of the last century (see Section 2.2 for details, and also supporting information Figure S1 for summary of the analysis steps and underlying data sets used in this study).

We considered an ensemble of Global Climate Models (GCMs) simulations from the archive of the Coupled Model Intercomparison Project 5 (CMIP5; Taylor et al., 2012) to estimate the projected changes in dry and wet extremes under the warming climate. As a majority of the CMIP5-GCMs do not have skills to simulate key features of the Indian summer monsoon, the selection of better performing GCMs is essential (Aadhar &

Mishra, 2019). Based on the extensive evaluation of CMIP5-GCMs for representing the south Asian monsoon characteristics by Ashfaq et al. (2017), we selected the six best performing GCMs (BNU-ESM, CESM1-CAM5, MIROC-ESM-CHEM, GFDL-ESM 2M, MPI-ESM-LR, and NorESM1-M) for our analysis. The performance of these GCMs was evaluated for several summer monsoon characteristics, as reported by Ashfaq et al. (2017). These well-performing GCMs have been also used for other hydrologic applications in the previous studies (Aadhar & Mishra, 2019, 2020).

We analyzed 240-years long simulations from the CMIP5-GCMs covering the period from 1861 to 2100 with historical and future simulations being considered as (1861–2005) and (2006–2100), respectively. We considered the two representative concentration pathways (RCPs) for the future projections corresponding to the moderate (RCP 4.5) and the highest emission (RCP8.5) scenarios for which all relevant variables (e.g., precipitation, temperature, radiation components, vapor pressure, and wind) were available. As all the required variables are available from the CMIP5-GCMs, we estimated PET using the modified Penman-Monteith method (Yang et al., 2019) that considers the changes in surface resistance (resistance of vapor flow through stomata openings) with varying atmospheric CO_2 concentration in the warming conditions. PET based on the modified Penman-Monteith method can be estimated as

$$\mathrm{PET} = \frac{0.408\Delta(\mathrm{R_n} - \mathrm{G}) + \gamma\frac{900}{T + 273}\mathrm{uD}}{\Delta + \gamma[1 + \mathrm{u}\{0.34 + 2.4 + 10^{-4}([\mathrm{CO_2}] - 300)\}]}$$

where R_n is net radiation at the surface, G is heat flux, Δ is the slope of the vapor pressure curve, u is wind speed, D is vapor pressure deficit, $[CO_2]$ is the global mean atmospheric CO_2 concentration and γ is psychometric constant.

We used gridded population data available at a 0.5° spatial resolution from the Center of Global Environmental Research (Murakami & Yamagata, 2019; www.cger.nies.go.jp/gcp/population-and-gdp.html) for the analysis of population affected by dry and wet extremes. This data set is developed considering spatial and economic interaction among cities and utilizes an ensemble learning technique to consider multiple auxiliary variables (e.g., road network, city population, and urban and agricultural areas) for downscaling countrywide population data to corresponding gridded estimates (Murakami & Yamagata, 2019). The data is available for 1980–2100 at a 10-year time interval. The data for 1980–2010 is based on the historical observations, while for 2020–2100 on the projected populations under three shared socioeconomic pathways (SSPs; O'Neill et al., 2017; van Vuuren et al., 2014): SSP1 (toward sustainability), SSP2 (middle-of-the-road scenario), and SSP3 (regional rivalry, the world is closed and fragmented into regions). The data set was further linearly interpolated to obtain the annual values to assist the analysis of extreme hydro-climatic conditions as described in Mishra et al. (2018). The SSPs provide future narratives describing different socioeconomic developments based among other things on populations, urbanization, technological and economic growths, and the different SSP scenarios, therefore, represents the high/low adaptation and mitigation challenges.

2.2. Estimation of Dry and Wet Extremes

We estimated the dry and wet extremes based on SPEI (Vicente-Serrano et al., 2010). SPEI characterizes the year-to-year variability of available water (the difference between precipitation and PET: P-PET) accumulated over any specified time intervals (e.g., month, season, or water-year). We estimated SPEI using the log-logistic distribution fitted to accumulated water (P-PET) over two timescales, representing the 4-months monsoon season (June–September) and the 12-months water-year (June–May), respectively. Similar to the well-known Standardized Precipitation Index (SPI; Mckee et al., 1993), SPEI varies between $[-\infty,\infty]$ with values above and below zero reflecting wet and dry conditions, respectively. A threshold value of 1.3, which corresponds to a return period of 10 years, was selected to represent the extreme dry (SPEI ≤ -1.3) and wet (SPEI ≥ 1.3) conditions, as these conditions would pose severe challenges to agriculture, water resources, and socioeconomic conditions in the affected regions (Shah & Mishra, 2015). Due to the varying length of observational and GCMs data sets, we used the period of 1951–2000 and 1861–2000 to deduce parameters of the fitted distribution for the observations and GCMs, respectively. While we note this methodological difference in the (fitting) time-period between both data sets, we emphasize that our goal here is not to compare outputs of two data sets (observations vs. GCMs), but rather to analyze the changes in the projected dry/wet extremes and the exposed population to the extreme conditions. Using

the long time-series of available water (P-PET) allowed us to robustly capture the form of the distribution function. Also, estimates of SPEI based on the long-term data can account for multi-decadal variability associated with summer monsoon rainfall (Shah & Mishra, 2016). As our analysis encompasses over a range of observational and GCM data sets with varying spatial resolutions, for the India-wide analysis, we re-gridded them to a standard grid of 1° spatial resolution. Similarly, for the estimation of historical and projected population affected to dry and wet extremes, we first aggregated the 0.5° population data set to a 1° spatial resolution and then counted the number of people falling within a specified extreme condition (dry/wet) across India.

We analyzed the changes in the spatial extent and population exposure in response to the global mean temperature rise of 1.5°C and 2°C above the preindustrial levels, which is in-line with the targeted temperature thresholds discussed in the 2015 Paris Agreement (UNFCC, 2015). Using the combination of GCMs and RCPs, we determined different levels of warming scenarios ranging from 0.5°C to 2.0°C temperature targets. In each of the warming world scenario, we then estimated the projected changes in the spatial extent and probability occurrence of wet and dry extremes in India. Next, using the projected population under different shared socioeconomic pathways (SSPs), we estimated the population exposed to both extremes under different warming levels. Figure S1 – as flow chart - depicts the main steps of analysis and underlying data sets used in this study.

2.3. Estimation of Global Warming Levels

We followed a time-sampling approach (James et al., 2017; Vautard et al., 2014) to estimate 30-year time-periods in the projected climate model simulations that correspond to different levels of global warming ranging from 0.5°C to 2.0°C above a preindustrial level. Using the three observation-based data sets of air temperature (from GISS LOTI, HadCRUT3, and NOAA-NCDC), James et al. (2017) reported the mean global warming of around 0.46°C for a reference period of 1971–2000 compared to the preindustrial period (1881–1910). We used this observation-based offset value (0.46°C) for the identification of the 30-year time periods corresponding to different warming levels from the CMIP5-GCM simulations. Furthermore, we used a range of 0.1°C to account for the uncertainty in the selection of a preindustrial period and the corresponding global mean temperature (Hawkins et al., 2017). For each GCM and RCP combination, we first referenced (subtracted) every projected 30-year global mean air temperature to their respective 1971–2000 estimates and then sampled all 30-year periods in which the global mean temperature of that GCM/RCP combination crossed a range of 0.99–1.09°C, 1.49–1.59°C, and 1.99–2.09°C for the warming levels of 1.0°C, 1.5°C, and 2.0°C, respectively. We also accounted for the uncertainty due to selection of a reference period (including the observational temperature estimates) by taking the samples of all 30-year period that correspond to warming levels of 0.46–0.51°C. Hereby the projected changes in the areal extent, occurrence, and population exposed to the wet and dry extremes under the warming climate using the GCMs/RCPs/SSPs are referenced to the historical simulation period of 1971–2000. We note the 30-year period (1971–2000) selected as the reference falls within the historical periods of the CMIP5-GCM simulations, which has been commonly used to represent the contemporary (reference) climate condition in the several climate change impact assessment studies (see, e.g., IPCC, 2018, SR1.5 report; Jacob et al., 2018; Mishra et al., 2017; Samaniego et al., 2018; Singh & Kumar, 2019; Vautard et al., 2014).

3. Results and Discussion

3.1. Observed Changes in the Area Affected by Dry and Wet Extremes

First, we estimated the changes in the areal extent of observed dry and wet extremes between 1951 and 2015 using the non-parametric Mann-Kendall test and Sen's slope method (Figures 1a and 1b), The area under dry (SPEI ≤ -1.3) and wet (SPEI ≥ 1.3) extremes were estimated for the summer monsoon season (June–September) and the water-year (June–May) timescales using the four observational precipitation products to account for uncertainty due to choice of different rainfall data sets (Lin & Huybers, 2019; Mishra, 2015; Singh et al., 2019). Uncertainty in the observed precipitation products can vary spatially based on the number of rain gauge stations (Prakash, 2019). Figure 1 shows the yearly evolution of area under dry and wet extremes in the monsoon season over the last six decades in India based on four (IMD, GPCC, CRU, and UDEL) precipitation data sets (see the corresponding water-year based extremes is shown in Figure S3). The area under dry extremes has significantly (p value < 0.05) increased at a rate of approximately 1% per

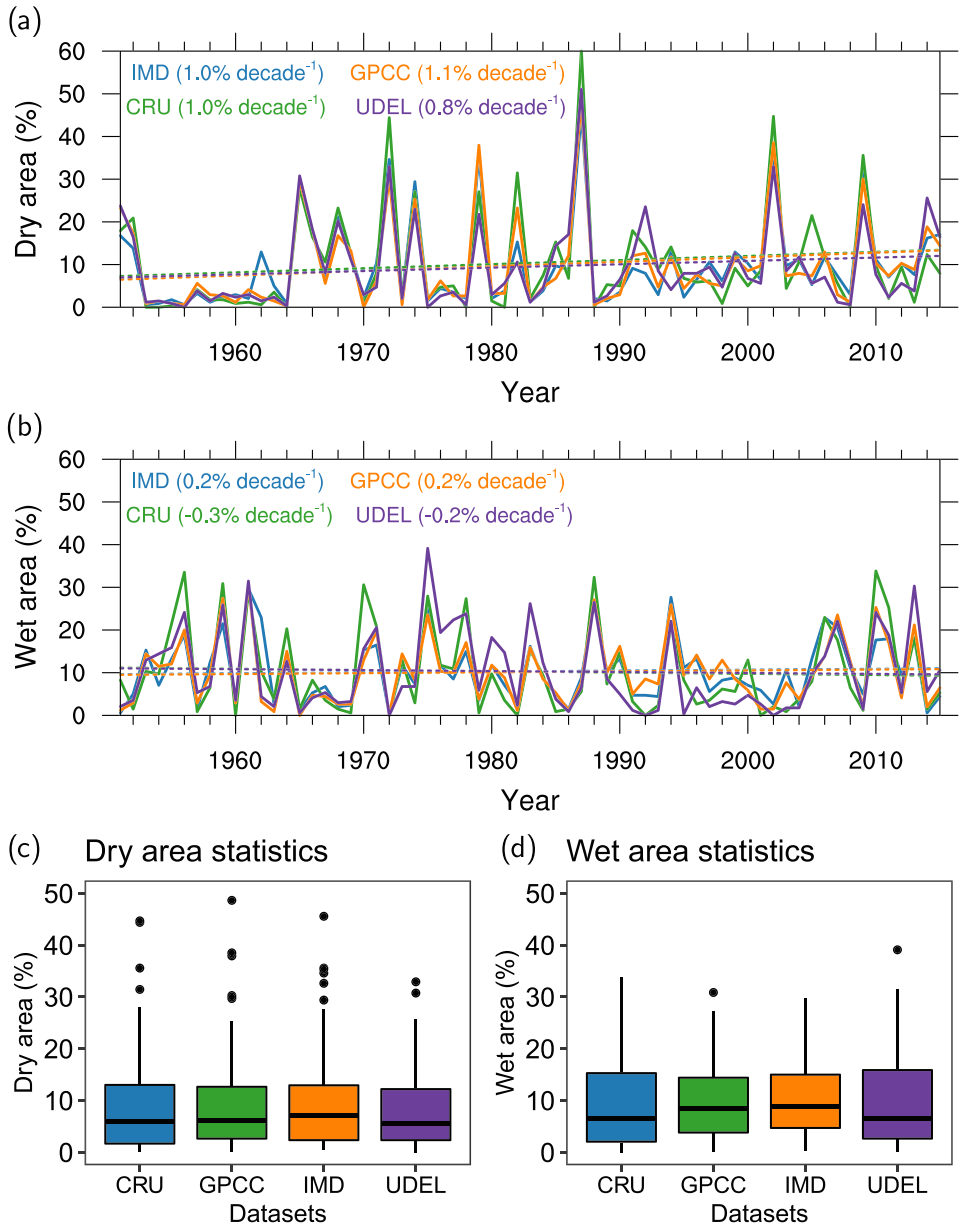

Figure 1. Annual evolution of the India area (in % of total land mass) under the (a) dry and (b) wet extremes estimated based on four observational data sets (CRU, GPCC, IMD, and UDEL) for the period 1950–2015. Dry and wet extremes are calculated based on 4 months (JJAS) monsoon season Standardized Precipitation-Evapotranspiration Index (SPEI) crossing a threshold value of + 1.3 (and above for wet) and − 1.3 (and below for dry). Panels (c) and (d) summarize the yearly estimates of the dry and wet areas as a box-plot diagram corresponding to the four data sets.

decade during the 1951–2015 period in India based on the IMD observations (Figures 1a and 1c). Increase in the area under the dry extremes in the IMD observations is consistent in the other three data sets (Figures 1a and 1c). For instance, CRU, GPCC, and UDEL also showed an increase of about 0.8–1.1% per decade during the 1951–2015 period. The temporal consistency of area under dry extremes among the four data sets is well correlated (Figure S2). For instance, the correlation between the area under dry extremes in IMD and CRU, GPCC, and UDEL are 0.91, 0.96, and 0.90, respectively (Figure S2). In general, all the four observation-based rainfall data sets show an increase in the area under dry extremes during the monsoon season during 1951–2015 in India (Figures 1a and 1c). Similar changes showing an increase in the area under dry extremes (0.5–1.0% per decade) and consistency among the four precipitation products are observed from the 12-months (water year) SPEI analysis (Figures S3 and S4).

Next, we examined the changes in the area affected by wet extremes (SPEI ≥ 1.3) using the four observational data sets during the 1951–2015 period (Figures 1b and 1d). Based on the IMD and GPCC data sets, the area affected by the wet extremes during the monsoon season in India has increased at a rate of 0.2% per decade over the last six decades (Figure 1b). Over the same period, the other two data sets (CRU and UDEL) show a declining trend in the area under wet extremes (−0.2% to −0.3% per decade). However, none of these changes is statistically significant at even 10% of the significance level. We find that the temporal agreement among the four data sets for the area under wet extremes is relatively low compared to that of dry extremes (Figure S2). Wet extremes during the summer monsoon season are often localized and occur at much smaller spatial scales than the dry extremes, which have a comparatively larger spatial footprint. Therefore, observational uncertainty in the area of wet extremes based on the four data sets is relatively higher (Figure S2). We find that the area under wet extremes using the 12-months (water year) based SPEI analysis has also not changed significantly during the 1951–2015 (Figure S3); as well the consistency among four precipitation products for the wet extremes being lower than that of dry extremes (Figure S4).

Over the past decades, dry and wet extreme years have affected different regions in India. The years in which more than 20% (one-fifth) of the country was affected by the dry and wet extremes were identified during 1951–2015 (Figure 2a). The top five dry extremes occurred during the summer monsoon season of 1972, 1979, 1987, 2002, and 2009 (Figure 2a). The dry extremes in these 5 years affected different parts of the country. For instance, dry extremes in 1987 and 2002 were more prominent in western India and affected nearly 45% and 35% of India, respectively. In contrast, the dry extremes during 1979 and 2009 were mostly centered on the Indo-Gangetic Plain. They covered nearly 36% and 33% of the country, respectively. Dry extremes in the monsoon season of 1972 affected a large part of northern and peninsular India with the coverage of about 35%. We analyzed the large-scale SST patterns corresponding to the dry (and wet) extremes observed across India using the observed sea surface temperature (SST) data set from the Met Office Hadley Centre UK (HadISST v1.1; Rayner et al., 2003) for the monsoon season (Wu et al., 2012). Composite SST anomalies were constructed for all the dry extremes (8 to 10 events depending on the data sets; see Figure 1a) that affected more than 20% of India during 1951–2015 in the observations from IMD (Figure 2c). The composite analysis shows that these dry extremes were associated with the warmer SST anomalies over the tropical Pacific, south Atlantic, and Indian Oceans (Figure 2c). Specifically, the relationship between warmer SST anomalies in the Pacific Ocean (Niño 3.4 region) and dry extremes during the summer monsoon in India is statistically significant at the 5% significance level (based on the *t* test).

The coupling between the Indian summer monsoon and the positive phase of El Niño Southern Oscillations (ENSO) is well known and has been discussed in detail in the previous studies (Kumar et al., 1999, 2007; Mishra et al., 2012; Wu et al., 2012). The decline in the summer monsoon precipitation after the middle of the last century has been observed primarily centered around the Indo-Gangetic Plain, which has been attributed to the stronger Indian Ocean warming (Mishra et al., 2012; Roxy et al., 2015). The composite analysis for the dry extremes over India based on other three observational products (CRU, GPCC, and UDEL) showed similar patterns of SST anomalies with that found for the IMD data set (Figure S5).

The top five wet extreme years covering more than one-fifth (20%) of the country occurred in 1961, 1975, 1988, 1994, and 2006 based on IMD observations (Figure 2b). Similar to dry extremes, wet extremes also exhibited considerable spatial variability. For instance, wet extremes of 1994 and 2006 affected western and central India with an aerial coverage of around 28% and 23%, respectively. The wet extreme of 1961 summer monsoon season affected central India and Indo-Gangetic Plain while in 1988 a large part of northern and peninsular India witnessed wet extremes. Nearly 26% of the country was affected by the wet extreme during the summer monsoon season in 1975 (Figure 2b). Similar to the dry extremes, we constructed composite of SST anomalies during the monsoon season for all the wet extreme years that covered more than 20% of the country during 1951–2015 (8 to 13 events depending on the data sets; see Figure 1b). Wet extremes are generally associated with the cooler SST anomalies over the central Pacific region (Figure 2d). The composite SST analysis of the wet extremes based on the other three (CRU, GPCC, and UDEL) data sets is consistent with that found for the IMD data set (Figure S4). Overall, our results show that the significant part of India can be affected by wet and dry extremes, which can pose tremendous pressure on water resources, agriculture, and infrastructure (Piao et al., 2010; Wheeler & Science, 2013).

10.1029/2020EF001731

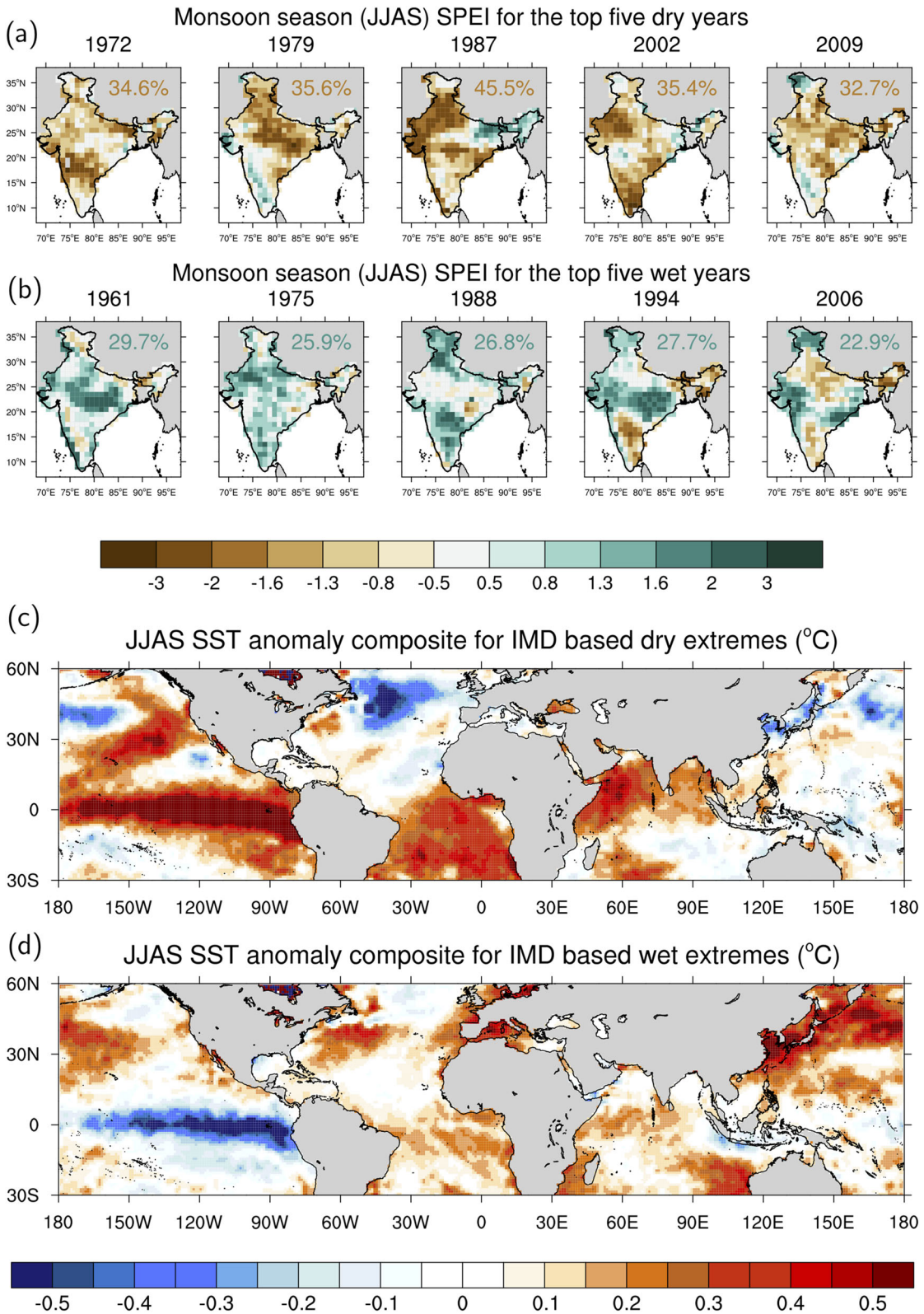

Figure 2. Spatial distribution of top five (a) dry and (b) wet extremes across India based on the monsoon season SPEI from the observation-based IMD data set during 1951–2015. Panels (c) and (d) show the composite of the JJAS Sea Surface Tempertaure (SST) anomalies corresponding to the topmost dry and wet extreme years, exceeding 20% of the spatial coverage across India. The SST anomalies are derived using climatology over the period 1951–2015 from the HadISST database (Rayner et al., 2003).

3.2. Projected Changes in Dry and Wet Extremes

We used simulations from the CMIP5-GCMs to understand the projected changes in the area affected by the dry and wet extremes in India. Using the six better performing CMIP5-GCMs, we estimated the projected changes in the 30-year mean global air temperature and the corresponding area under dry/wet extremes across India in the 21st century under the moderate (RCP4.5) and the high (RCP8.5) emission scenarios (Figure 3a). The changes under the projected climate were referenced to the historical period (1971–2000). The selected climate models project an increase in the global mean temperature of about 2.0°C ± 0.5°C (mean ± one standard deviation) and 3.75°C ± 0.75°C under the RCP 4.5 and RCP 8.5 scenarios, respectively, by the end of the 21st century (2071–2100; Figure 3a). The difference of nearly 2°C between these two scenarios may have a substantial influence on the occurrence and spatial extent of dry and wet extremes in India.

There is a large inter-model variation in the projections of the area under dry extremes in India, specifically under RCP8.5 from the middle of the 21st century (Figures 3a and S6). This uncertainty in the projected area under the dry extremes can be attributed to the differences in the CMIP5-GCMs and their ability to simulate the Indian summer monsoon (Menon et al., 2013). There are also differences in the projected area under dry extremes between the two RCPs scenarios. While the CMIP5-GCMs project a slight decline in the area affected by the dry extremes during the summer monsoon season under RCP4.5 by the end of the 21st century (from 9.6 ± 3.2% in 1971–2000 to 9.3 ± 3.8% in 2071–2100), the models project on average an increase in the area affected by the dry extremes under the RCP8.5 (14.5 ± 8.4% in 2071–2100). The divergence between the projections under the two RCPs starts around the middle of the 21st century. On the other side, the area under the wet extremes in India is overall to rise under both scenarios in the warming climate (Figure 3a). The projected increase in the area under the wet extremes during the monsoon season by end of the 21st century in India is nearly same in both future scenarios: from 10.4 ± 2.3% in 1971–2000 to 19.1 ± 5.2% under RCP4.5 and 19.4 ± 6.3% under RCP8.5 in 2071–2100. Results of the water-year SPEI based projected changes in the wet and dry extreme areas are consistently similar to those of the above-noted changes for the monsoon season (Figure S6).

Next, we analyzed the sensitivity of different global warming levels above the preindustrial level on the projected changes in the dry and wet extremes across India. To this end, we estimated probability ratio (PR; Fischer & Knutti, 2015; Stott et al., 2004) as the ratio of the probability of occurrence of the dry/wet extremes in the warmer world (1.5°C or 2.0°C) to the probability of the dry/wet extremes in the reference period of 1971–2000 (Figures 3b–3e). The ensemble-averaged PR of the dry extremes estimated based on the combination of GCMs/RCPs is higher than the one in the large part of the country (~85%) indicating an increase in the occurrence of dry extremes during the summer monsoon under the 1.5°C and 2.0°C warmer worlds (Figure 3b; see also Figure S6 for results corresponding to water-year based SPEI analysis). A large part of central and peninsular India, as well as Indo-Gangetic Plain, is projected to experience on average an increase in the occurrence of the dry extreme under the warming climate (Figure 3b). About 15% of the country is projected to experience at-least twice the occurrence of the dry extremes (PR ≥ 2) under the (1.5°C and 2.0°C) warmer worlds. We, however, find that the uncertainty in the projected increase in the dry extremes based on the coefficient of variation (CV) of PRs under the warming climate is generally high (with CV > 1) especially in northwest India, which shows that there is relatively large disagreement among the GCMs (Figure 3d). In large part of India (>80%), the CV (PR) values are generally lesser than 1, indicating a moderate signal to noise ratio (i.e., a moderate agreement among the GCMs). We find a stronger agreement among the GCM projections for the PR estimates (i.e., CV ≤ 0.5) over nearly 20% of the country under the warmer worlds.

Similar to the PR of dry extremes, the PR of wet extremes is projected to increase in large part of the country under the 1.5°C and 2.0°C warmer worlds (Figure 3c). Nearly 81–84% of the country is projected to experience PR higher than one while about 20–22% of the country is likely to witness PR more than two (i.e., twice the occurrence probability of extreme wet monsoon years) under the warmer worlds. Compared to the dry extremes, there is a higher agreement among the CMIP5-GCMs on the projected increase in the wet extremes under the warming climate with nearly 95% of the study area exhibited CV (PR) less than 1 (Figure 3e). The future projections on the occurrence of the dry extremes reveal a high inter-model uncertainty, which is attributable to the uncertainty in the precipitation projections in

10.1029/2020EF001731

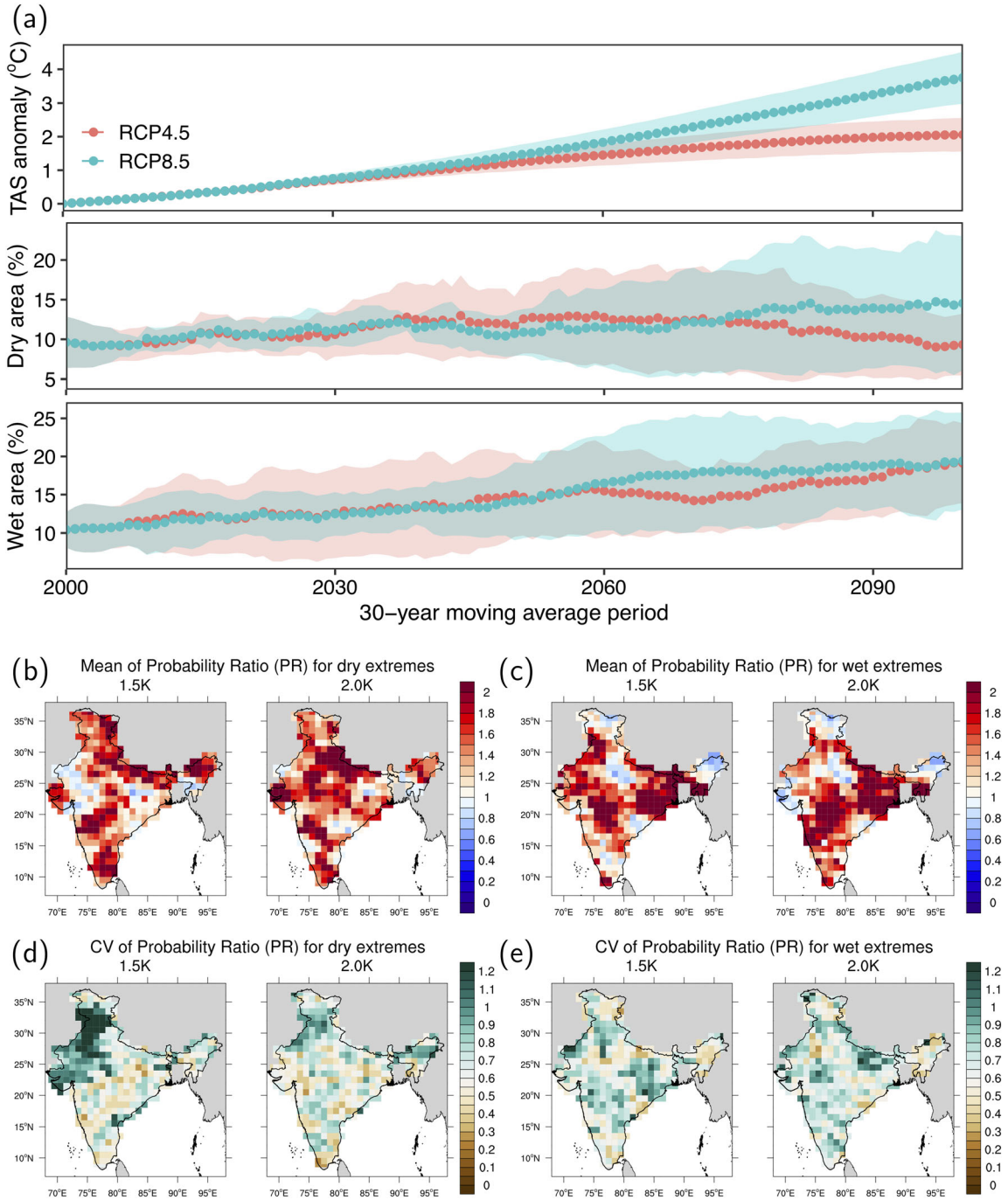

Figure 3. (a) Ensemble mean and spread (standard deviation) of 30-year moving averages of the global surface temperature (TAS) anomaly referenced to the baseline period of 1971–2000, and area under dry (SPEI ≤ −1.3) and wet (SPEI ≥ 1.3) extremes across India for the period 2000–2100 under two RCP scenarios (4.5 and 8.5). Bottom panels show the corresponding (b, c) ensemble mean and (d, e) coefficient of variation (CV) of the probability ratios (PR) illustrating the spatial changes in dry and wet extremes across India under the 1.5 and 2.0 K (or °C) warmer worlds. PR in warming periods is referenced to the historical period 1971–2000.

India (Mishra et al., 2014; Singh & AchutaRao, 2018). The summer monsoon season precipitation is projected to increase in India under the warming climate (Chaturvedi et al., 2012; Kumar et al., 2006; Menon et al., 2013). However, changes in the monsoon season precipitation in India under the warming climate are associated with the uncertainty (Turner & Annamalai, 2012) as the global and regional climate models still do not simulate underlying process reasonably well (Kitoh et al., 2013; Shepherd, 2014;

10.1029/2020EF001731

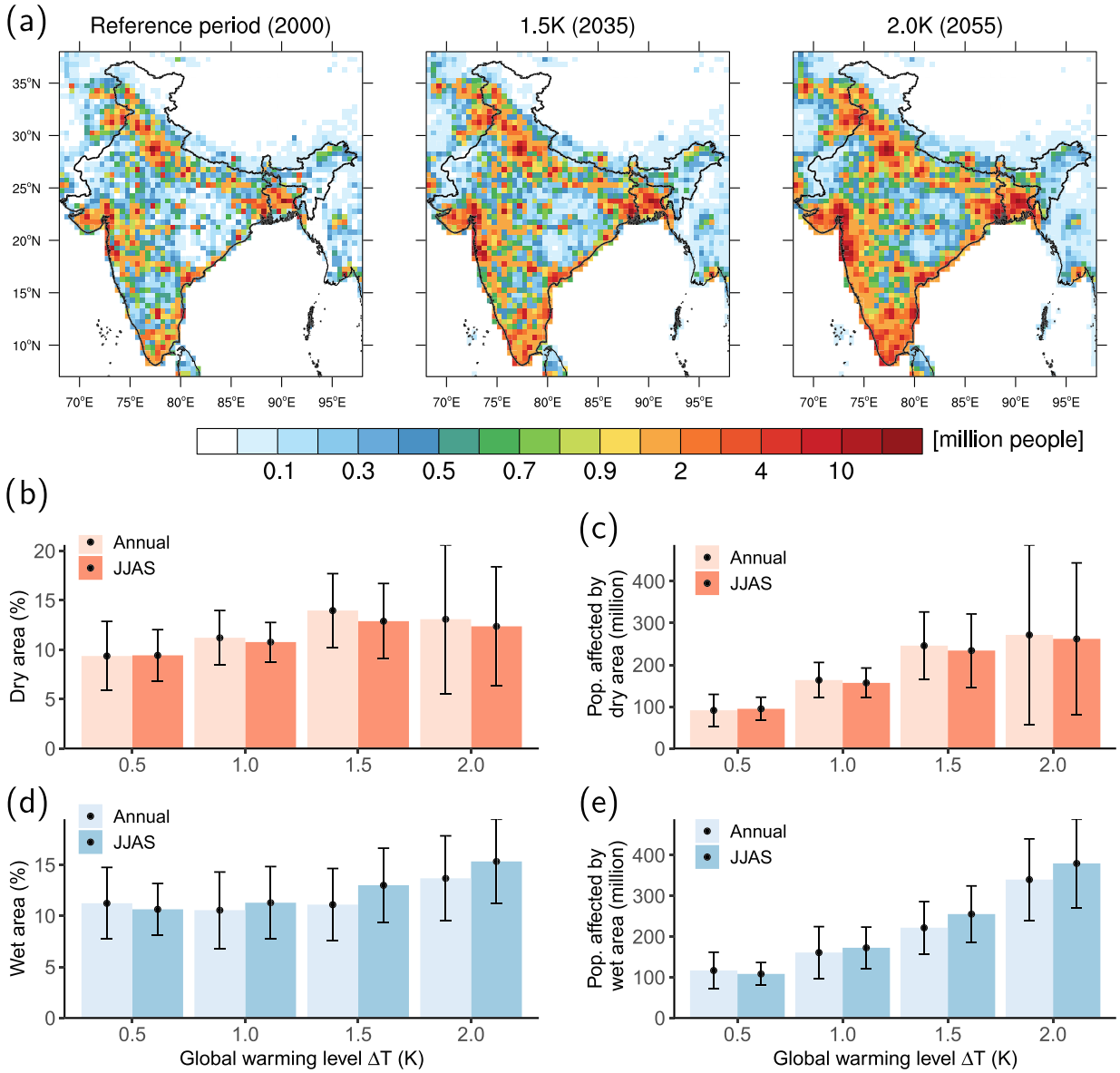

Figure 4. (a) Spatial distribution of historical and projected changes in population across India under the SSP3 scenario (the corresponding plots for SSPs 1 and 2 are shown in Figure S7). (b, d) Bar plot (in the left) shows the mean areal extent (and error bars as one standard deviation) of India area under the dry and wet extremes for different global warming levels; $\Delta T = 0.5$–2.0 K(or °C) and (c, e) the corresponding changes in population that are projected to be affected under the dry and wet extremes across India under the SSP3 scenario (see Figure S7 for the corresponding plots for SSPs 1 and 2). The error bars showing the uncertainty are estimated based on samples for each of the warmer world scenario that consists of an ensemble of GCMs, RCPs, and sampling uncertainty (i.e., ±0.05°C around the reference estimate for determining the preindustrial temperature levels; see Method for more details).

Sperber et al., 2013). Nonetheless, the risk of extreme dry and wet events during the summer monsoon season in India remains plausible under the warming climate (Krishnan et al., 2016; Mukherjee et al., 2018).

3.3. Projected Spatial Extent and Population Exposure to Dry and Wet Extremes

We examined the projected changes in the area and corresponding population exposed by the dry and wet extremes in India under different global warming level targets (0.5–2.0°C). The population is projected to increase under the 1.5°C and 2.0°C warmer worlds in large part of the country under all the three SSP scenarios (SSP1, SSP2, and SSP3) (Figure 4a for SSP3; and Figures S7a and S7b for SSP1 and SSP2, respectively). A few regions (Gangetic Plain, western India, and southern India) are projected to experience a higher

increase in the population than the other parts of the country (Figures 4a, S7a, and S7b). Climate change mitigation may be beneficial in reducing the area affected by the dry and wet extremes in India under the warming climate (Figures 4b and 4d). On average, the area affected by the dry extremes in the summer monsoon season under the 1.5°C warming level is slightly (0.5%) lower than that estimated for the 2.0°C warming level (Figure 4b). Nevertheless, compared to the reference period estimates, the climate models projected an increase in the area affected by the dry extremes in India under both 1.5°C and 2.0°C warmer worlds (i.e., from roughly 9.5% in the reference period to 13% and 12.5% in the 1.5°C and 2.0°C warmer worlds, respectively). Similarly, the area under the wet extremes is also projected to increase under the warming world (from nearly 10% in the reference period to 13% and 15.5% at the 1.5°C and 2.0°C worlds, respectively). Furthermore, the projected area affected by the wet extremes under the 1.5°C warming world is about 2.5% lower than the area if the global mean temperature rises to 2.0°C (Figure 4d). This reflects the added benefits of limiting the global temperature rise to 1.5°C above the preindustrial level as discussed in the 2015 Paris meeting (UNFCC, 2015). Overall the combined area affected by the dry and wet extremes for the summer monsoon season in India is projected to increase around 26–28% under the 1.5–2.0°C warmer worlds. The analysis for the water year also depicts a consistent picture of increase in the area affected by dry and wet extremes in India, similar to that of the monsoon season changes under the warming climate (Figures 4d and S7).

The above-noted projected increase in the area under the dry and wet extremes can pose enormous pressure on millions of people of India. We find that about 139–167 million more people will be exposed to the (summer monsoon) dry extremes if the global mean temperature increases 1.5°C or 2.0°C above the preindustrial level (Figure 4c). On the other side, about 147–271 million more people are projected to be exposed to the wet extremes in India under the warmer worlds (Figure 4e). The population exposed to the combined dry and wet extremes in India is projected to increase by twofold to threefold under the 1.5°C to 2.0°C warmer worlds (i.e., on average from 203 million people in the reference period to 489 and 641 million people in the 1.5°C and 2.0°C warmer worlds). These population projections correspond to the SSP3 scenario, which is consistent with the future world projected under higher emission scenarios. The other two SSP scenarios also show similarly increased population exposure to the dry and wet extremes in India under the warming climate (Figures S7d and S7f). Our results show a substantial reduction in population exposure (around 150 million people) to the dry and wet extremes by limiting the global warming to 1.5°C temperature target compared to the 2.0°C (Figures 4c and 4e). We emphasize that the impact of the climate warming on population exposure due to the dry and wet extremes is consistently higher under the 2.0°C world despite a slightly lower area being affected by the dry extremes in India under the 1.5°C world compared to the 2.0°C world. The demographical changes of increasing population in India under different SSP scenarios predominantly governs the projected exposed population to wet and dry extremes (Figures 4a and S7). Besides the higher population exposure to extremes, the projected rise in the combined dry and wet extremes across India in the 21st century will have serious implications on agriculture, water resources, and infrastructure and can cause substantial economic losses.

4. Summary

The rapidly growing economy and infrastructure in India are likely to face an increased risk under the warming climate due to rise in the extreme precipitation events (Ali et al., 2018; Goswami et al., 2006; Mukherjee et al., 2018; Roxy et al., 2017). The recent flood events in Kerala and Uttarakhand have had remarkable impacts on all aspects of socioeconomic lives. Furthermore, recent droughts in India hampered food and freshwater security in large parts of the country as witnessed during the drought of 2015–2016 (Mishra et al., 2016). We report that the combined area under the extreme dry and wet events during the summer monsoon season has substantially increased over the long-term record of 1951–2015, which is consistent across different observational data sets. Also consistent with the observational changes, the CMIP5-GCMs project a considerable increase in the area affected by the dry and wet extremes in India. A significant proportion of the India population is projected to be exposed to the dry and wet extremes in the future. We find that climate change mitigation, especially limiting the global mean temperature below 1.5°C from the preindustrial level, can significantly reduce the population exposure to the dry and wet extremes in India.

Data Availability Statement

Data sets used in this study are freely available from India Meteorological Department (http://dsp.imdpune.gov.in/), CRU (https://crudata.uea.ac.uk/cru/data/hrg/), University of Delaware (https://psl.noaa.gov/data/gridded/data.UDel_AirT_Precip.html), GPCC (https://psl.noaa.gov/data/gridded/data.gpcc.html), HadISST(https://www.metoffice.gov.uk/hadobs/hadisst/), and SSPs (www.cger.nies.go.jp/gcp/population-and-gdp.html). The CMIP5 model output can be accessed through the Earth System Grid Federation (ESGF) gateways.

Acknowledgments

VM acknowledge the funding from BELMONT Forum and the Ministry of Earth Sciences. The data availability from IMD and other observational sources as well the CMIP5 simulations and SSPs data sets are greatly appreciated. We acknowledge the World Climate Research Programme's Working Group on Coupled Modelling, which is responsible for CMIP, and we thank the climate modeling groups (listed in Table XX of this paper) for producing and making available their model output. For CMIP the U.S. Department of Energy's Program for Climate Model Diagnosis and Intercomparison provides coordinating support and led development of software infrastructure in partnership with the Global Organization for Earth System Science Portals. UDel_AirT_Precip data provided by the NOAA/OAR/ESRL PSL, Boulder, Colorado, USA, from their Web site at https://psl.noaa.gov/. GPCC Precipitation data provided by the NOAA/OAR/ESRL PSL, Boulder, Colorado, USA, from their Web site at https://psl.noaa.gov/. Finally, we thank the editor and two anonymous reviewers for their valuable and constructive feedback that helped to improve the original manuscript. Open access funding enabled and organized by Projekt DEAL.

References

Aadhar, S., & Mishra, V. (2019). A substantial rise in the area and population affected by dryness in South Asia under 1.5°C, 2.0°C and 2.5°C warmer worlds. *Environmental Research Letters*, *14*, 114021. https://doi.org/10.1088/1748-9326/ab4862

Aadhar, S., & Mishra, V. (2020). Increased drought risk in South Asia under warming climate: Implications of uncertainty in potential evapotranspiration estimates. *Journal of Hydrometeorology*. https://doi.org/10.1175/JHM-D-19-0224.1

Alfieri, L., Burek, P., Feyen, L., & Forzieri, G. (2015). Global warming increases the frequency of river floods in Europe. *Hydrology and Earth System Sciences Discussions*, *12*(1), 1119–1152. https://doi.org/10.5194/hess-19-2247-2015

Ali, H., Modi, P., & Mishra, V. (2019). Increased flood risk in Indian sub-continent under the warming climate. *Weather and Climate Extremes*, *25*, 100212. https://doi.org/10.1016/j.wace.2019.100212

Ali, S. A., Aadhar, S., Shah, H. L., & Mishra, V. (2018). Projected increase in hydropower production in India under climate change. *Scientific Reports*, *8*, 12450. https://doi.org/10.1038/s41598-018-30489-4

Allen, R. G., Pereira, L. S., Raes, D., & Smith, M. (1998). *Crop evapotranspiration: Guidelines for computing crop water requirements*, *Irrigation and Drainage Paper* (Vol. 56). Rome: Food and Agric. Org., U. N.

Ashfaq, M., Rastogi, D., Mei, R., Touma, D., & Leung, L. R. (2017). Sources of errors in the simulation of south Asian summer monsoon in the CMIP5 GCMs. *Climate Dynamics*, *49*, 193–223. https://doi.org/10.1007/s00382-016-3337-7

Barnett, T. P., Adam, J. C., & Lettenmaier, D. P. (2005). Potential impacts of a warming climate on water availability in snow-dominated regions. *Nature*, *438*, 303–309. https://doi.org/10.1038/nature04141

Becker, A., Finger, P., Meyer-Christoffer, A., Rudolf, B., Schamm, K., Schneider, U., & Ziese, M. (2013). A description of the global land-surface precipitation data products of the Global Precipitation Climatology Centre with sample applications including centennial (trend) analysis from 1901-present. *Earth System Science Data*, *5*(1), 71–99. https://doi.org/10.5194/essd-5-71-2013

Berghuijs, W. R., Aalbers, E. E., Larsen, J. R., Trancoso, R., & Woods, R. A. (2017). Recent changes in extreme floods across multiple continents. *Environmental Research Letters*, *12*, 114035. https://doi.org/10.1088/1748-9326/aa8847

Chaturvedi, R. K., Joshi, J., Jayaraman, M., & Bala, G. (2012). Multi-model climate change projections for India under representative concentration pathways. *Current Science*, *103*(7), 791–802. https://doi.org/10.2307/24088836

Cook, B. I., Ault, T. R., & Smerdon, J. E. (2015). Unprecedented 21st century drought risk in the American Southwest and Central Plains. *Science Advances*, *1*, e1400082. https://doi.org/10.1126/sciadv.1400082

Dai, A. (2013). Increasing drought under global warming in observations and models. *Nature Climate Change*, *3*(1), 52–58. https://doi.org/10.1038/nclimate1633

Diffenbaugh, N. S., Swain, D. L., & Touma, D. (2015). Anthropogenic warming has increased drought risk in California. *Proceedings of the National Academy of Sciences*, *112*(13), 3931–3936. https://doi.org/10.1073/pnas.1422385112

Dottori, F., Szewczyk, W., Ciscar, J.-C., Zhao, F., Alfieri, L., Hirabayashi, Y., et al. (2018). Increased human and economic losses from river flooding with anthropogenic warming. *Nature Climate Change*, *8*(9), 781–786. https://doi.org/10.1038/s41558-018-0257-z

Fischer, E. M., & Knutti, R. (2015). Anthropogenic contribution to global occurrence of heavy-precipitation and high-temperature extremes. *Nature Climate Change*, *5*(6), 560–564. https://doi.org/10.1038/nclimate2617

Garg, S., & Mishra, V. (2019). Role of extreme precipitation and initial hydrologic conditions on floods in Godavari River Basin, India. *Water Resources Research*, *55*, 9191–9210. https://doi.org/10.1029/2019WR025863

Goswami, B. N., Venugopal, V., Sengupta, D., Madhusoodanan, M. S., & Xavier, P. K. (2006). Increasing trend of extreme rain events over India in a warming environment. *Science*, *314*(5804), 1442–1445. https://doi.org/10.1126/science.1132027 Retrieved from, http://science.sciencemag.org/content/314/5804/1442

Gudmundsson, L., Leonard, M., Do, H. X., Westra, S., & Seneviratne, S. I. (2019). Observed trends in global indicators of mean and extreme streamflow. *Geophysical Research Letters*, *46*, 756–766. https://doi.org/10.1029/2018GL079725

Hallegatte, S., Green, C., Nicholls, R. J., & Corfee-Morlot, J. (2013). Future flood losses in major coastal cities. *Nature Climate Change*, *3*, 802–806. https://doi.org/10.1038/nclimate1979

Hargreaves, G. H., & Samani, Z. A. (1985). Reference crop evapotranspiration from temperature. *Applied Engineering in Agriculture*, *1*, 96–99. https://doi.org/10.13031/2013.26773

Harris, I. C., & Jones, P. D. (2019). CRU TS4.02: Climatic Research Unit (CRU) Time-Series (TS) version 4.02 of high-resolution gridded data of month-by-month variation in climate (Jan. 1901- Dec. 2017). Centre for Environmental Data Analysis, 01 April 2019. https://doi.org/10.5285/b2f81914257c4188b181a4d8b0a46bff

Harris, I., Osborn, T. J., Jones, P., & Lister, D. (2020). Version 4 of the CRU TS monthly high-resolution gridded multivariate climate dataset. *Scientific Data*, *7*, 109. https://doi.org/10.1038/s41597-020-0453-3

Hawkins, E., Ortega, P., Suckling, E., Schurer, A., Hegerl, G., Jones, P., et al. (2017). Estimating changes in global temperature since the preindustrial period. *Bulletin of the American Meteorological Society*, *98*, 1841–1856. https://doi.org/10.1175/BAMS-D-16-0007.1

Huntingford, C., Marsh, T., Scaife, A. A., Kendon, E. J., Hannaford, J., Kay, A. L., et al. (2014). Potential influences on the United Kingdom's floods of winter 2013/14. *Nature Climate Change*, *4*, 769–777. https://doi.org/10.1038/nclimate2314

Immerzeel, W. W., Van Beek, L. P. H., & Bierkens, M. F. P. (2010). Climate change will affect the Asian water towers. *Science*, *328*(5984), 1382–1385. https://doi.org/10.1126/science.1183188

IPCC (2018). Global warming of 1.5°C. An IPCC Special Report on the Impacts of Global Warming of 1.5°C above Preindustrial Levels and Related Global Greenhouse Gas Emission Pathways, in the Context of Strengthening the Global Response to the Threat of Climate Chang. IPCC-World Meteorol. Organ Geneva.

Jacob, D., Kotova, L., Teichmann, C., Sobolowski, S. P., Vautard, R., Donnelly, C., et al. (2018). Climate impacts in Europe under + 1.5°C global warming. *Earth's Future*, *6*, 264–285. https://doi.org/10.1002/2017EF000710

James, R., Washington, R., Schleussner, C. F., Rogelj, J., & Conway, D. (2017). Characterizing half-a-degree difference: A review of methods for identifying regional climate responses to global warming targets. *Wiley Interdisciplinary Reviews: Climate Change*, *8*, e457. https://doi.org/10.1002/wcc.457

Jin, Q., & Wang, C. (2017). A revival of Indian summer monsoon rainfall since 2002. *Nature Climate Change*, *7*(8), 587–594. https://doi.org/10.1038/nclimate3348

Jongman, B., Hochrainer-Stigler, S., Feyen, L., Aerts, J. C. J. H., Mechler, R., Botzen, W. J. W., et al. (2014). Increasing stress on disaster-risk finance due to large floods. *Nature Climate Change*, *4*, 264–268. https://doi.org/10.1038/nclimate2124

Kitoh, A., Endo, H., Krishna Kumar, K., Cavalcanti, I. F. A., Goswami, P., & Zhou, T. (2013). Monsoons in a changing world: A regional perspective in a global context. *Journal of Geophysical Research: Atmospheres*, *118*, 3053–3065. https://doi.org/10.1002/jgrd.50258

Krishna Kumar, K., Rupa Kumar, K., Ashrit, R. G., Deshpande, N. R., & Hansen, J. W. (2004). Climate impacts on Indian agriculture. *International Journal of Climatology*, *24*(11), 1375–1393. https://doi.org/10.1002/joc.1081

Krishnamurthy, V., & Shukla, J. (2000). Intraseasonal and interannual variability of rainfall over India. In *Journal of Climate* (Vol. *13*, pp. 4366–4377). American Meteorological Society. https://doi.org/10.1175/1520-0442(2000)013<0001:IAIVOR>2.0.CO;2

Krishnan, R., Sabin, T. P., Vellore, R., Mujumdar, M., Sanjay, J., Goswami, B. N., et al. (2016). Deciphering the desiccation trend of the South Asian monsoon hydroclimate in a warming world. *Climate Dynamics*, *47*(3–4), 1007–1027. https://doi.org/10.1007/s00382-015-2886-5

Kumar, R., & Acharya, P. (2016). Flood hazard and risk assessment of 2014 floods in Kashmir Valley: a space-based multisensor approach. *Natural Hazards*, *84*(1), 437–464. https://doi.org/10.1007/s11069-016-2428-4

Kumar, K. K., Rajagopalan, B., & Cane, M. A. (1999). On the weakening relationship between the Indian monsoon and ENSO. *Science* (New York, N.Y., *284*(5423), 2156–2159. https://doi.org/10.1126/SCIENCE.284.5423.2156

Kumar, K. R., Sahai, A. K., Kumar, K. K., Patwardhan, S. K., Mishra, P. K., Revadekar, J. V., et al. (2006). High-resolution climate change scenarios for India for 21st century. *Current Science*, *90*(3), 334–346. Retrieved from http://repository.ias.ac.in/67506/1/67506.pdf

Kumar, P., Rupa Kumar, K., Rajeevan, M., & Sahai, A. K. (2007). On the recent strengthening of the relationship between ENSO and northeast monsoon rainfall over South Asia. *Climate Dynamics*, *28*(6), 649–660. https://doi.org/10.1007/s00382-006-0210-0

Legates, D. R., & Willmott, C. J. (1990). Mean seasonal and spatial variability in gauge-corrected, global precipitation. *International Journal of Climatology*, *10*(2), 111–127. https://doi.org/10.1002/joc.3370100202

Lesk, C., Rowhani, P., & Ramankutty, N. (2016). Influence of extreme weather disasters on global crop production. *Nature*, *259*, 84–87. https://doi.org/10.1038/nature16467

Lin, M., & Huybers, P. (2019). If rain falls in India and no one reports it, are historical trends in monsoon extremes biased? *Geophysical Research Letters*, *46*, 1681–1689. https://doi.org/10.1029/2018GL079709

Lobell, D. B., & Field, C. B. (2007). Global scale climate-crop yield relationships and the impacts of recent warming. *Environmental Research Letters*, *2*, 014002. https://doi.org/10.1088/1748-9326/2/1/014002

Mckee, T. B., Doesken, N. J., & Kleist, J. (1993). The relationship of drought frequency AND duration to time scales. In *Proceedings of the 8th Conference on Applied Climatology Conference on Applied Climatology* (Vol. 17, pp. 179–184). Boston: American Meteorological Society.

Menon, A., Levermann, A., Schewe, J., Lehmann, J., & Frieler, K. (2013). Consistent increase in Indian monsoon rainfall and its variability across CMIP-5 models. *Earth System Dynamics*, *4*(2), 287–300. https://doi.org/10.5194/esd-4-287-2013

Mishra, V. (2015). Climatic uncertainty in Himalayan water towers. *Journal of Geophysical Research: Atmospheres*, *120*, 2689–2705. https://doi.org/10.1002/2014JD022650

Mishra, V., Aaadhar, S., Shah, H., Kumar, R., Pattanaik, D. R., & Tiwari, A. D. (2018). The Kerala flood of 2018: Combined impact of extreme rainfall and reservoir storage. *Hydrology and Earth System Sciences Discussions*, 1–13. https://doi.org/10.5194/hess-2018-480

Mishra, V., Aadhar, S., Asoka, A., Pai, S., & Kumar, R. (2016). On the frequency of the 2015 monsoon season drought in the Indo-Gangetic Plain. *Geophysical Research Letters*, *43*, 12,102–12,112. https://doi.org/10.1002/2016GL071407

Mishra, V., Kumar, D., Ganguly, A. R., Sanjay, J., Mujumdar, M., Krishnan, R., & Shah, R. D. (2014). Reliability of regional and global climate models to simulate precipitation extremes over India. *Journal of Geophysical Research: Atmospheres*, *119*, 9301–9323. https://doi.org/10.1002/2014JD021636

Mishra, V., Mukherjee, S., Kumar, R., & Stone, D. A. (2017). Heat wave exposure in India in current, 1.5°C, and 2.0°C worlds. *Environmental Research Letters*, *12*, 124012. https://doi.org/10.1088/1748-9326/aa9388

Mishra, V., Smoliak, B. V., Lettenmaier, D. P., & Wallace, J. M. (2012). A prominent pattern of year-to-year variability in Indian summer monsoon rainfall. *Proceedings of the National Academy of Sciences*, *109*(19), 7213–7217. https://doi.org/10.1073/pnas.1119150109

Mishra, V., Thirumalai, K., Singh, D., & Aadhar, S. (2020). Future exacerbation of hot and dry summer monsoon extremes in India. *Npj Climate and Atmospheric Science*, *3*, 10. https://doi.org/10.1038/s41612-020-0113-5

Mishra, V., Tiwari, A. D., Aadhar, S., Shah, R., Xiao, M., Pai, D. S., & Lettenmaier, D. (2019). Drought and famine in India, 1870–2016. *Geophysical Research Letters*, *46*, 2075–2083. https://doi.org/10.1029/2018GL081477

Mukherjee, S., Aadhar, S., Stone, D., & Mishra, V. (2018). Increase in extreme precipitation events under anthropogenic warming in India. *Weather and Climate Extremes*, *20*, 45–53. https://doi.org/10.1016/J.WACE.2018.03.005

Mukherjee, S., & Mishra, V. (2018). A sixfold rise in concurrent day and night-time heatwaves in India under 2°C warming. *Scientific Reports*, *8*, 16922. https://doi.org/10.1038/s41598-018-35348-w

Murakami, D., & Yamagata, Y. (2019). Estimation of gridded population and GDP scenarios with spatially explicit statistical downscaling. *Sustainability* (Switzerland) *11*, 2106. https://doi.org/10.3390/su11072106

O'Neill, B. C., Kriegler, E., Ebi, K. L., Kemp-Benedict, E., Riahi, K., Rothman, D. S., et al. (2017). The roads ahead: Narratives for shared socioeconomic pathways describing world futures in the 21st century. *Global Environmental Change*, *42*, 169–180. https://doi.org/10.1016/j.gloenvcha.2015.01.004

Pai, D. S., Sridhar, L., Rajeevan, M., Sreejith, O. P., Satbhai, N. S., & Mukhopadyay, B. (2014). Development of a new high spatial resolution (0.25° × 0.25°) long period (1901–2010) daily gridded rainfall data set over India and its comparison with existing data sets over the region. *Mausam*, *65*(1), 1–18.

Parida, Y. (2020). Economic impact of floods in the Indian states. *Environment and Development Economics*, *25*(3), 267–290. https://doi.org/10.1017/S1355770X19000317

Parida, Y., Saini, S., & Chowdhury, J. R. (2020). Economic growth in the aftermath of floods in Indian states. *Environment, Development and Sustainability*, 1–27. https://doi.org/10.1007/s10668-020-00595-3

Peng, S., Huang, J., Sheehy, J. E., Laza, R. C., Visperas, R. M., Zhong, X., et al. (2004). Rice yields decline with higher night temperature from global warming. *Proceedings of the National Academy of Sciences*, *101*, 9971–9975. https://doi.org/10.1073/pnas.0403720101

Perkins, S. E., Alexander, L. V., & Nairn, J. R. (2012). Increasing frequency, intensity and duration of observed global heatwaves and warm spells. *Geophysical Research Letters*, *39*, L20714. https://doi.org/10.1029/2012GL053361

Piao, S., Ciais, P., Huang, Y., Shen, Z., Peng, S., Li, J., et al. (2010). The impacts of climate change on water resources and agriculture in China. *Nature*, *467*(7311), 43–51. https://doi.org/10.1038/nature09364

Prakash, S. (2019). Performance assessment of CHIRPS, MSWEP, SM2RAIN-CCI, and TMPA precipitation products across India. *Journal of Hydrology*, *571*, 50–59. https://doi.org/10.1016/j.jhydrol.2019.01.036

Ray, K., Pandey, P., Pandey, C., Dimri, A. P., & Kishore, K. (2019). On the recent floods in India. *Current Science*, *117*(2), 204. https://doi.org/10.18520/cs/v117/i2/204-218

Rayner, N. A., Parker, D. E., Horton, E. B., Folland, C. K., Alexander, L. V., Rowell, D. P., et al. (2003). Global analyses of sea surface temperature, sea ice, and night marine air temperature since the late nineteenth century. *Journal of Geophysical Research*, *108*(D14), 4407. https://doi.org/10.1029/2002JD002670

Roxy, M. K., Ghosh, S., Pathak, A., Athulya, R., Mujumdar, M., Murtugudde, R., et al. (2017). A threefold rise in widespread extreme rain events over central India. *Nature Communications*, *8*, 708. https://doi.org/10.1038/s41467-017-00744-9

Roxy, M. K., Ritika, K., Terray, P., Murtugudde, R., Ashok, K., & Goswami, B. N. (2015). Drying of Indian subcontinent by rapid Indian Ocean warming and a weakening land-sea thermal gradient. *Nature Communications*, *6*, 7423. https://doi.org/10.1038/ncomms8423

Samaniego, L., Thober, S., Kumar, R., Wanders, N., Rakovec, O., Pan, M., et al. (2018). Anthropogenic warming exacerbates European soil moisture droughts. *Nature Climate Change*, *8*, 421–426. https://doi.org/10.1038/s41558-018-0138-5

Schewe, J., Heinke, J., Gerten, D., Haddeland, I., Arnell, N. W., Clark, D. B., et al. (2014). Multimodel assessment of water scarcity under climate change. *Proceedings of the National Academy of Sciences*, *111*(9), 3245–3250. https://doi.org/10.1073/pnas.1222460110

Schneider, U., Becker, A., Finger, P., Meyer-Christoffer, A., & Ziese, M. (2018). GPCC Full Data Monthly Product Version 2018 at 1.0°: Monthly land-surface precipitation from rain-gauges built on GTS-based and historical data. Global Precipitation Climatology Centre. https://doi.org/10.5676/DWD_GPCC/FD_M_V2018_100

Shah, H. L., & Mishra, V. (2016). Hydrologic changes in Indian sub-continental river basins (1901–2012). *Journal of Hydrometeorology*, *17*(10), 2667–2687. https://doi.org/10.1175/JHM-D-15-0231.1

Shah, R. D., & Mishra, V. (2015). Development of an experimental near-real-time drought monitor for India. *Journal of Hydrometeorology*, *16*(1), 327–345. https://doi.org/10.1175/JHM-D-14-0041.1

Sharma, A., Wasko, C., & Lettenmaier, D. P. (2018). If precipitation extremes are increasing, why aren't floods? *Water Resources Research*, *54*, 8545–8551. https://doi.org/10.1029/2018WR023749

Shepherd, T. G. (2014). Atmospheric circulation as a source of uncertainty in climate change projections. *Nature Geoscience*, *7*(10), 703–708. https://doi.org/10.1038/NGEO2253

Singh, D., Ghosh, S., Roxy, M. K., & McDermid, S. (2019). Indian summer monsoon: Extreme events, historical changes, and role of anthropogenic forcings. *Wiley Interdisciplinary Reviews: Climate Change*, *10*, e571. https://doi.org/10.1002/wcc.571

Singh, D., Tsiang, M., Rajaratnam, B., & Diffenbaugh, N. S. (2014). Observed changes in extreme wet and dry spells during the South Asian summer monsoon season. *Nature Climate Change*, *4*(6), 456–461. https://doi.org/10.1038/nclimate2208

Singh, R., & AchutaRao, K. (2018). Quantifying uncertainty in twenty-first century climate change over India. *Climate Dynamics*, *52*(7–8), 3905–3928. https://doi.org/10.1007/s00382-018-4361-6

Singh, R., & Kumar, R. (2019). Climate versus demographic controls on water availability across India at 1.5°C, 2.0°C and 3.0°C global warming levels. *Global and Planetary Change*, *177*, 1–9. https://doi.org/10.1016/j.gloplacha.2019.03.006

Sperber, K. R., Annamalai, H., Kang, I. S., Kitoh, A., Moise, A., Turner, A., et al. (2013). The Asian summer monsoon: An intercomparison of CMIP5 vs. CMIP3 simulations of the late 20th century. *Climate Dynamics*, *41*, 2711–2744. https://doi.org/10.1007/s00382-012-1607-6

Stott, P. A., Stone, D. A., & Allen, M. R. (2004). Human contribution to the European heatwave of 2003. *Nature*, *432*(7017), 610–614. https://doi.org/10.1038/nature03089

Taylor, K. E., Stouffer, R. J., & Meehl, G. A. (2012). An overview of CMIP5 and the experiment design. *Bulletin of the American Meteorological Society*, *93*, 485–496. https://doi.org/10.1175/BAMS-D-11-00094.1

Trenberth, K. E., Dai, A., van der Schrier, G., Jones, P. D., Barichivich, J., Briffa, K. R., & Sheffield, J. (2014). Global warming and changes in drought. *Nature Climate Change*, *4*(1), 17–22. https://doi.org/10.1038/NCLIMATE2067

Turner, A. G., & Annamalai, H. (2012). Climate change and the South Asian summer monsoon. *Nature Climate Change*, *2*, 587–595. https://doi.org/10.1038/nclimate1495

Udmale, P. D., Ichikawa, Y., Manandhar, S., Ishidaira, H., Kiem, A. S., Shaowei, N., & Panda, S. N. (2015). How did the 2012 drought affect rural livelihoods in vulnerable areas? Empirical evidence from India. *International Journal of Disaster Risk Reduction*, *13*, 454–469. https://doi.org/10.1016/j.ijdrr.2015.08.002

UNFCC (2015). Adoption of the Paris agreement, Proposal by the President Technical Report. Geneva: United Nations (http://unfccc.int/resource/docs/2015/cop21/eng/l09r01.pdf)

van Vuuren, D. P., Kriegler, E., O'Neill, B. C., Ebi, K. L., Riahi, K., Carter, T. R., et al. (2014). A new scenario framework for climate change research: Scenario matrix architecture. *Climatic Change*, *122*(3), 373–386. https://doi.org/10.1007/s10584-013-0906-1

Vautard, R., Gobiet, A., Sobolowski, S., Kjellström, E., Stegehuis, A., Watkiss, P., et al. (2014). The European climate under a 2°C global warming. *Environmental Research Letters*, *9*, 034006. https://doi.org/10.1088/1748-9326/9/3/034006

Vicente-Serrano, S. M., Beguería, S., & López-Moreno, J. I. (2010). A multiscalar drought index sensitive to global warming: The standardized precipitation evapotranspiration index. *Journal of Climate*, *23*(7), 1696–1718. https://doi.org/10.1175/2009JCLI2909.1

Ward, P. J., Jongman, B., Weiland, F. S., Bouwman, A., Van Beek, R., Bierkens, M. F. P., et al. (2013). Assessing flood risk at the global scale: Model setup, results, and sensitivity. *Environmental Research Letters*, *8*, 044019. https://doi.org/10.1088/1748-9326/8/4/044019

Wheeler, T., & Science, J. V. B. (2013). Climate change impacts on global food security. Science.Sciencemag.Org.

Winsemius, H. C., Aerts, J. C. J. H., Van Beek, L. P. H., Bierkens, M. F. P., Bouwman, A., Jongman, B., et al. (2016). Global drivers of future river flood risk. *Nature Climate Change*, *6*, 381–385. https://doi.org/10.1038/nclimate2893

Wu, R., Chen, J., & Chen, W. (2012). Different types of ENSO influences on the Indian summer monsoon variability. *Journal of Climate*, *25*, 903–920. https://doi.org/10.1175/JCLI-D-11-00039.1

Yang, Y., Roderick, M. L., Zhang, S., McVicar, T. R., & Donohue, R. J. (2019). Hydrologic implications of vegetation response to elevated CO_2 in climate projections. *Nature Climate Change*, *9*, 44–48. https://doi.org/10.1038/s41558-018-0361-0

10.1029/2020EF001731

Erratum

In the originally published version of this paper, the X and Y axis of figure 1c and 1d were missing. This error has since been corrected and this version may be considered the authoritative version of record.